RSC Advances

RSC Publishing

PAPER

View Article Online
View Journal | View Issue

Cite this: *RSC Advances*, 2013, **3**, 2404

A reagent based DOS strategy *via* Evans chiral auxiliary: highly stereoselective Michael reaction towards optically active quinolizidinones, piperidinones and pyrrolidinones†

Subhabrata Sen,*[a] Siva R. Kamma,[ab] Rambabu Gundla,[a] Uma Adepally,[b] Santosh Kuncha,[b] Sridhar Thirnathi[a] and U. Viplava Prasad[c]

Received 11th September 2012,
Accepted 12th December 2012

DOI: 10.1039/c2ra22115b

www.rsc.org/advances

In the present study, we have demonstrated the diversity oriented synthesis of nitrogen heterocycles *viz.* chiral piperidinones, quinolizidinones and diaryl pyrrolidinones from Michael adducts generated *via* a $TiCl_4$-catalyzed highly stereoselective Michael reaction with nitrostyrenes and an Evans chiral auxiliary. We also reported a Cu-4,4′-(isopropyl)-substituted isopropylidene-bridged 2,2′-bis-1,3′-oxazoline catalyst mediated catalytic asymmetric version of this reaction. *In silico* analysis is utilized to evaluate the diversity of the set of compounds against shape space (PMI), polar surface area (PSA) calculations and relevant drug like properties (*viz.* HBA, HBD, PSA, mol. wt., log P and log D). Finally, the molecules were screened against microorganisms to assess their antimicrobial properties.

Introduction

Chemical synthesis of small molecules has recently undergone a paradigm shift (including the evolving area of diversity-oriented synthesis (DOS)) in the generation of an architecturally diverse set of organic molecules for the identification of new ligands for a variety of biological targets.[1] The diversity oriented synthetic (DOS) methodology utilized a combination of building block-, appendage-, stereochemical-, and skeletal-diversity to access structurally unique compounds.[2] Among these, skeletal diversity is the most difficult to achieve, and at the same time is considered the most useful technique, because it provides distinct molecular scaffolds that occupy different regions of chemical space.[3] Skeletal diversity is commonly achieved either by (a) a substrate-based approach that employs a common set of reagents to elaborate functionally and structurally unique precursors or (b) a reagent-based method that utilizes a common intermediate that when subjected to a variety of reaction conditions or reagents, affords different scaffolds.[4] In this article we have demonstrated the utility of this reagent-based approach as a DOS strategy by the preparation of multiple heterocyclic scaffolds.

Piperidinone, quinolizidinone and pyrrolidinone motifs are key structural subunits of naturally occurring biologically active molecules.[5–7] They are abundant among complex alkaloid natural products and are used as key intermediates for the synthesis of a variety of pharmaceutical candidates. Hence, we were interested in strategizing a DOS based methodology for these kinds of scaffolds. These scaffolds adhere to the *rule of three* as closely as possible ($M < 300$; HBD $\leqslant 3$ and HBA $\leqslant 3$; clogP = 3; number of rotatable bonds $\leqslant 3$; polar surface area = 60 Å^2). These parameters are generally accepted to be the most appropriate in creating fragment libraries.[8] Both linear racemic and chiral synthesis of these scaffolds have been reported in the past.[9] However, to the best of our knowledge, this is the first reagent-based enantioselective DOS methodology that allows access to these structurally diverse molecular scaffolds through the common chiral imides **1, 10–12 and 14** (Scheme 1). In this regard, we report a highly stereoselective $TiCl_4$ catalyzed Evans–Michael reaction, with a variety of nitrostyrenes, to generate the key intermediates **2**, **15–21** and **23**. We achieved skeletal diversity on these *via* an asymmetric cascade reaction with cyclic and acyclic imines (to generate the chiral piperidinone and quinolizidinone scaffolds), and *in situ* hydrogenation and lactamization (to generate the chiral diaryl pyrrolidinones). Facile removal of the chiral auxiliary (Evans' oxazolidinone) makes this an extremely efficient asymmetric pathway to access these

[a]*Plot 28A, IDA Nacharam, Hyderabad, India. E-mail: subhabrata.sen@gvkbio.com; organic6@hotmail.com; Fax: 91 40 2715 2999; Tel: 91 40 6628 1529*
[b]*Institute of Science and Technology, JNTU Kukatpally, Hyderabad, Andhra Pradesh, India*
[c]*Department of Organic Chemistry and FDW, Andhra University, Vizag, India. E-mail: viplav_31049@yahoo.com*

† Electronic supplementary information (ESI) available. CCDC 899422. For ESI and crystallographic data in CIF or other electronic format see DOI: 10.1039/c2ra22115b

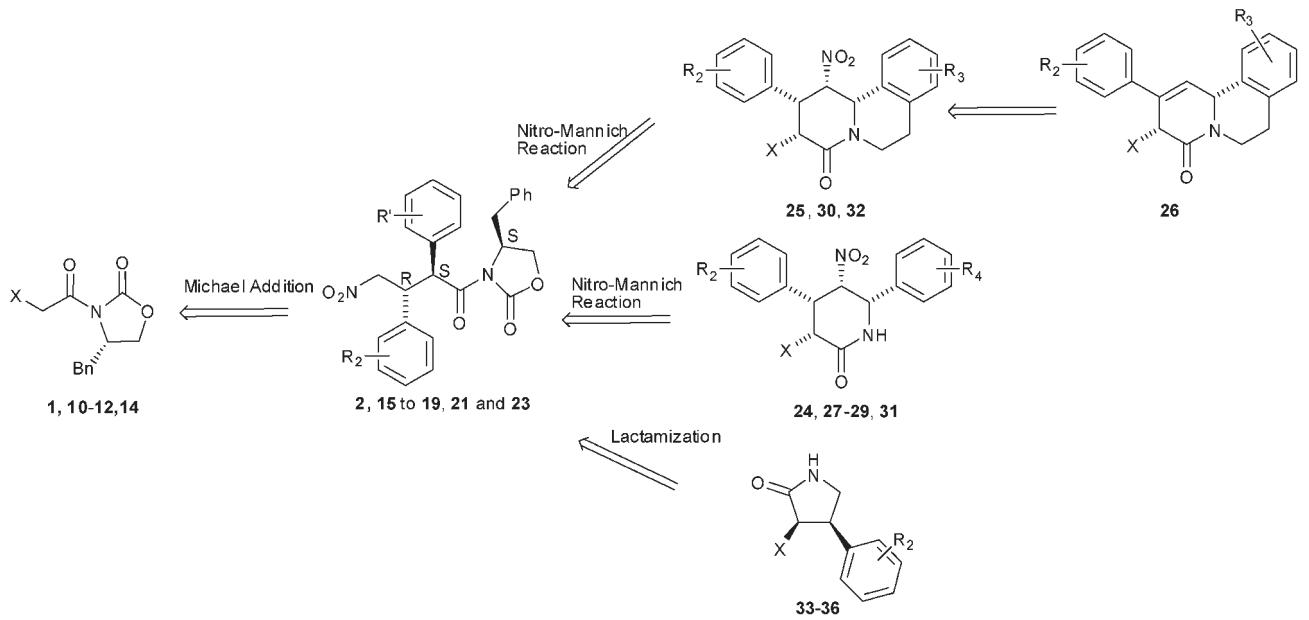

Scheme 1 Diversity oriented synthesis of N-heterocycles.

scaffolds. We also demonstrated a successful catalytic asymmetric version of Michael addition and amination on the achiral analog **13** with a Cu-4,4'-(isopropyl)-substituted isopropylidene-bridged 2,2'-bis-1,3'-oxazoline catalyst (Scheme 2).

The highlight of our methodology is a 2-step synthesis of three distinct natural product-inspired scaffolds. The methodology also executed *via* the catalytic asymmetric Michael addition has an attractive *steps-per-scaffold efficiency* to provide access to chemically complex molecules. We further evaluated our scaffolds *via in silico* studies, followed by screening them against five pathogens.

Results and discussion

The key starting material **1** was synthesized *via* a literature protocol.[10a]

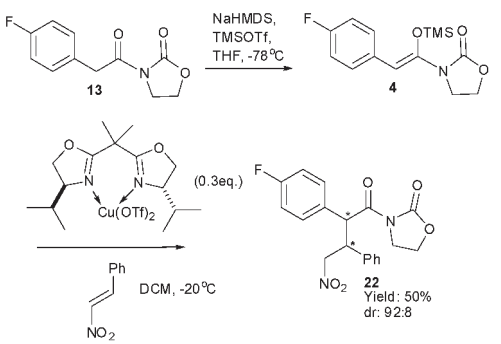

Scheme 2 Catalytic asymmetric Michael reaction.

To optimize the Michael addition, **1** was treated with nitrostyrene in THF in the presence of various bases and temperatures (Table 1). With a mild base like potassium carbonate (K_2CO_3, 1.2 equiv.) in THF at room temperature no

Table 1 Michael reaction of nitrostyrenes

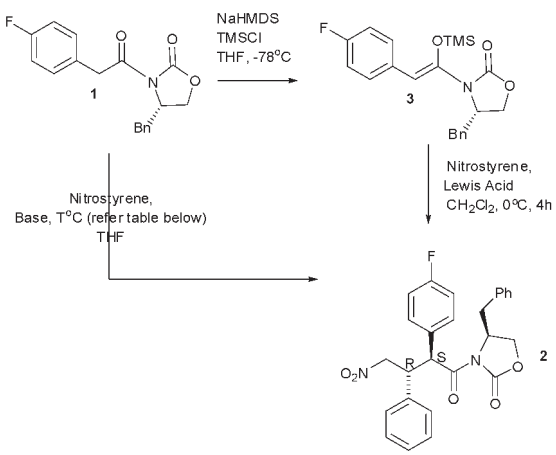

No.	Base (equiv.)	T (°C)	Lewis acid	Yield (%)[a]	dr[b]
1	K_2CO_3 (1.2 eq.)	rt	—	0	0
2	NaH (1.2 eq.)	0–rt	—	43	60 : 40
3	LHMDS (1 eq.)	−78	—	48	62 : 38
4	KHMDS (1 eq.)	"	—	54	65 : 35
5	NaHMDS (1 eq.)	"	—	50	65 : 35
6	—	−78–0	BF_3-Et_2 (0.2)	56	80 : 20
7	—	−78–0	Et_2AlCl (0.2)	42	65 : 35
8	—	−78–0	$TiCl_4$ (0.1)	25	88 : 12
9	—	−78–0	$TiCl_4$ (0.3)	75	95 : 5

[a] Isolated yield. [b] Based on HPLC.

reaction was observed, while a significant amount of the unreacted starting material was detected by LC-MS (Table 1, entry 1). With NaH (1.2 equiv.) in THF (0 °C to rt) the desired product was obtained in a moderate yield (~43%) and poor diastereoselectivity (60%) (Table 1, entry 2). Bases such as LHMDS, KHMDS and NaHMDS (1.0 equiv.) (Table 1, entry 3–5) marginally improved the yield (48–54%) and diastereoselectivity (62–65%). These moderate results prompted us to search for better conditions for the reaction. We opted for a catalytic Lewis acid mediated procedure, where we converted the imide **1** to the corresponding silyl ketene imide **3** by TMSCl (TMSOTf can also enable a similar transformation), followed by *in situ* treatment with a series of Lewis acids ($TiCl_4$, BF_3-OEt_2 and Et_2AlCl) (0.1–0.25 equiv.) and 1 equiv. of nitrostyrene at 0 °C for 12 h. The summary of the results is shown in Table 1. BF_3-OEt_2 (0.2 equiv., entry 6) mediated Michael addition afforded **2** in a 56% yield and in a 80 : 20 diastereomeric ratio (dr). Et_2AlCl did not promote the reaction as efficiently (entry 7). The use of 0.1 equiv. of $TiCl_4$ caused a significant reduction of the yield (entry 8). Eventually, the best result of a 75% yield and a 95 : 5 dr was obtained when we employed 0.3 equiv. of $TiCl_4$ (entry 9).

To explore the generic nature of the titanium catalyzed procedure, a variety of nitro olefins were reacted with several chiral acyl oxazolidinones, **1**, **10–12** and **14**.[10b–e] The reaction conditions are in accordance with the optimized conditions in Table 1. We were pleased to observe the resulting Michael adducts, **2**, **15–21** and **23** in moderate to high yields (38–86%) and high dr (81 : 19 → 99 : 1). The results are summarized in Table 2.

Table 2 $TiCl_4$ catalyzed Michael addition of various nitro olefins with chiral oxazolidines

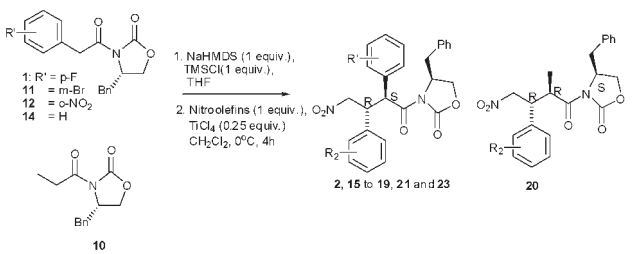

Entry[a]	Substrate	Product	Yield (%)[b]	dr[c]
1	**1**	**2**, R_2 = H	72	97 : 3
2	"	**15**, R_2 = *p*-OMe	57	95 : 5
3	"	**16**, R_2 = *o*-Cl	86	82 : 12
4	"	**17**, R_2 = *m*-OMe	38	99 : 1
5	**12**	**18**, R_2 = *p*-OMe	48	87 : 13
6	"	**19**, R_2 = H	69	97 : 3
7	**10**	**20**, R_2 = H	75	91 : 9
8	**11**	**21**, R_2 = H	81	88 : 12
9	**14**	**23**, R_2 = H	48	81 : 19

[a] Reaction conditions: imide (1.0 mmol), TMSCl (1.5 mmol), NaHMDS (1.0 mmol), THF (5 mL), $TiCl_4$ (0.3 mmol), 0 °C, 24 h. [b] Isolated yield. [c] Determined by HPLC (refer to the supplementary information).

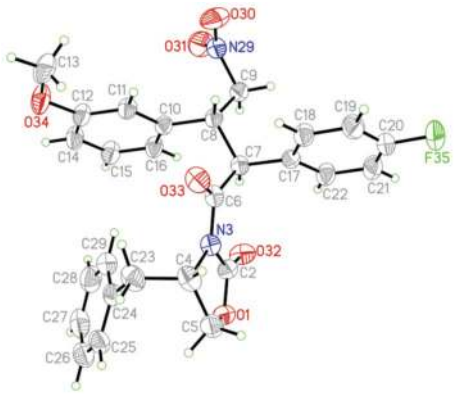

Fig. 1 X-ray crystal structure of compound **17**.

The absolute stereochemistry of the Michael adducts were determined by the single crystal X-ray of compound **17** (shown in Fig. 1 and Table 2).

A catalytic asymmetric version of the Michael reaction has also been developed, where **13** is converted to the corresponding silyl ketene imide **4**, which was then treated *in situ* with a Cu-4,4'-(isopropyl)-substituted isopropylidene-bridged 2,2'-bis-1,3'-oxazoline catalyst (0.3 equiv.) and nitrostyrene to generate the Michael adduct **22** in a 50% yield and with a 92% diastereoselectivity (Scheme 2). The results are yet to be optimized. We are presently investigating several other catalyst–ligand systems to improve the yields and the diastereoselectivity.

With the desired Michael adducts in hand, three distinct scaffolds were synthesized by applying a nitro-Mannich/lactamization cascade and *in situ* hydrogenation and lactamization. The nitro-Mannich/lactamization cascade constituted an extension of Mühlstädt's nitro-Mannich chemistry.[11] In this regard **2** and 3,4-dihydroisoquinoline were chosen as the reaction partners for the optimization study. The reactions

Table 3 Synthesis and optimization of the reaction conditions for quinolizidinones

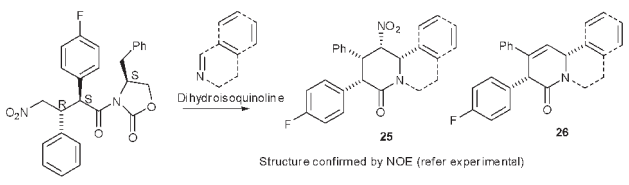

Entry	Solvents	Temp	Yield (%)[a]	dr[b]
1	Toluene		~4	—
2	IPA		18	67 : 33
3	THF		12	—
4	THF–H_2O (1 : 1)	reflux	28	—
5	H_2O	100 °C	25	88 : 12
6	H_2O	70 °C	71	95 : 5

[a] Isolated yields. [b] Diastereoselectivity.

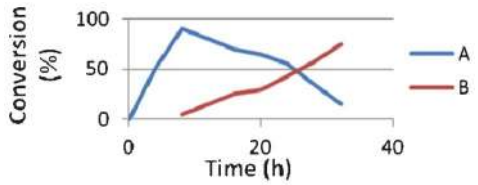

Fig. 2 Conversion of **25** to **26** over time.

were investigated in various solvents (overnight) (Table 3). At high temperatures in solvents like toluene and THF (entry 1 and 3, respectively), the reactions were sluggish (after 16 h, LCMS suggested a 4–12% conversion to the desired product). With isopropanol (IPA) (entry 2), the conversion was also very low with a 67 : 33 dr. On shifting the reaction to aqueous medium we observed ~28% of the desired product in 1 : 1 water–THF (under reflux) (entry 4). In water at 100 °C we observed about a 25% yield of the desired product with 88 : 12 dr (entry 5). Finally, we were pleased to isolate the desired quinolizidinone **24** in about a 71% yield and a 95 : 5 dr at ~70 °C in water in a sealed vessel for about 16 h (entry 6). Interestingly, we also observed the unsaturated analog **26** as the byproduct with the desired compound **25** (Table 3). On close monitoring of the reaction by HPLC, we observed that after about 7–10 h, ~90% of **25** (represented by graph A in Fig. 2) is formed, with about 5% of the unsaturated compound **26** (represented by graph B in Fig. 2).

After ~15 h, ~70% of **25** (plot A) and ~20% of **26** (plot B) are generated. On further heating, the unsaturated product **26** increased and after about 36 h the desired quinolizidinone **25** is completely converted to **26** (Fig. 2). In a similar approach, we obtained **33** along with **30**, and in a separate reaction **32** was

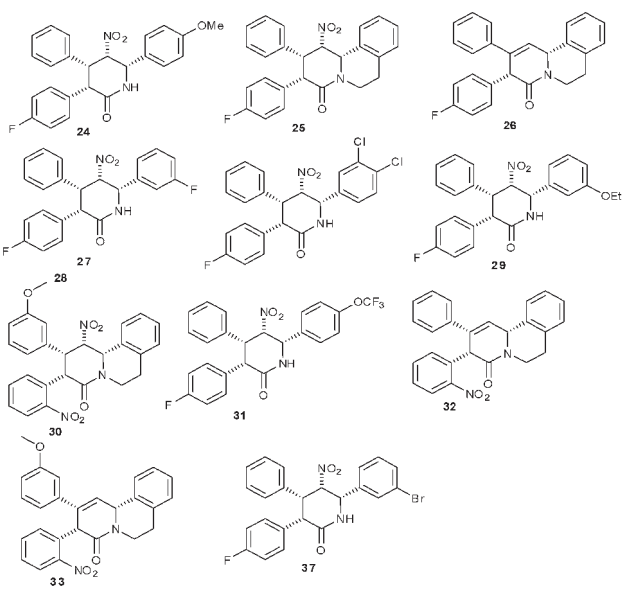

Fig. 3 Quinolizidinones and piperidinones.

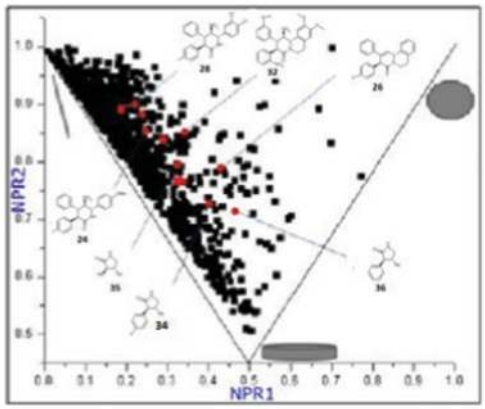

Fig. 4 Normalized ratios of principal moments of inertia plotted in two dimensional triangular graphs (NPR-analysis) using drug candidates and our compounds.

isolated as the single product by the prolonged heating of **19** with dihydroisoquinoline (Fig. 3).

Piperidinones **24**, **27–29**, **31** and **37** were successfully synthesized from imines I–V (generated *in situ* by reacting ammonium acetate with the appropriate aldehydes) by treating them with **2** in the presence of ethanol (Scheme 3). The absolute stereochemistry of the quinolizidinones/piperidinones were determined by NOE of the representative compound **24** (Fig. 3).[12]

A third class of heterocyclic compounds, pyrrolidinones **34–36**, were synthesized by converting the nitro adducts **2**, **15** and **23** by hydrogenation followed by *in situ* lactamization (Scheme 4).

With various scaffolds in hand we set out to evaluate the skeletal diversity that is afforded by the N-heterocycles and their related chemical descriptors, *via in silico* algorithms. By virtue of possessing its own set of drug like properties, each molecule possesses a unique point in the chemical space. Hence, the larger the span of coverage of the chemical space by a collection of molecules, the greater is their diversity. In order to assess the diversity of the reported compounds we plotted them in chemical space plots corresponding to a set of six drug like properties (PSA, solubility, HBA, HBD, log A and log D), relative to the 1011 FDA approved drugs as reported in the

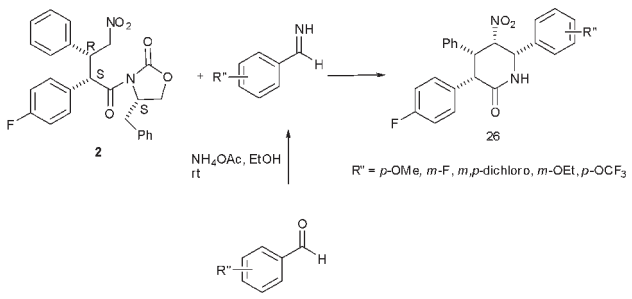

Scheme 3 Synthesis of the pyrrolidinones.

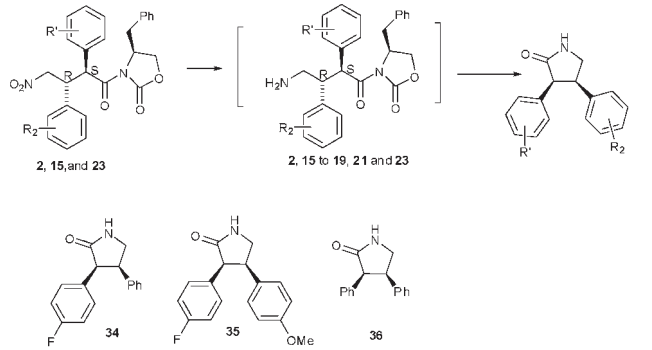

Scheme 4 Synthesis of the pyrrolidinones.

GOSTAR database.[13] The plots demonstrated that our collection of molecules covered a substantial area in the chemical space (Fig. 6). They also did not cluster together with the corresponding nitro adducts that they were derived from.

Additionally, quinolizidinones, piperidinones and pyrrolodinones were plotted according to the normalized principal moment of inertia (PMI) formalism of Sauer and Schwartz.[14] The molecular shape and biological activity are interconnected and correlated. The principal moments of inertia (PMI) is a topological descriptor and normalized ratios of the principal moments of inertia (NPR) can be considered to describe the molecular shape of the compounds. It is an expedient and visual way to showcase diversity corresponding to the area of chemical space covered by a collection of molecules.[14] A screening collection has a high degree of molecular shape diversity built in, which increases the probability of a wide range of biological activity. The PMI calculation involved aligning each molecule to the principal moment axes in SYBYL and then normalized PMI values were calculated by a software developed in-house.[15] In this regard Fig. 4 exhibits a large coverage of shape space for our N-heterocycles **24–32**, which were derived from the Michael adducts **2** and **15–23**, thereby demonstrating the diversity achieved by this methodology. Our collection of molecules can be segregated into three classes of scaffolds; piperidinones (**24**, **27**, **28**, **29**, **31**), quinolizidinones (**25**, **26**, **30**, **32** and **33**) and pyrrolidinones (**34–36**).

The plot demonstrates that the FDA approved drugs cover the left edge of the PMI space and so do our collection of molecules (taking shapes intermediate between rods and discs). They cover a wide area, thereby demonstrating the diversity achieved *via* our methodology.

In addition to shape, space and *in silico* analysis of the drug like properties, the polar surface area of a small molecule is also a relevant descriptor for diverse biologically active molecules involved in ligand–receptor binding. There are several reports where a different orientation of heteroatoms in a small molecule generates a diverse polar surface area. This results in a difference in response towards key covalent interactions *viz.* H-bonding and electrostatic interactions *etc.*, and in turn displays a diverse biological activity. Hence, polar surface areas of **25**, **26**, **32** and **34** (representing the different classes of scaffold) were plotted. Surface electrostatic profiles were calculated by projecting the Gasteiger–Marsili charge distribution onto a Connolly surface generated *via* the MOLCAD tool in SYBYL. The scaffolds we synthesized had a PSA that ranges between acceptable values of CNS and non-CNS orally active drugs. Fig. 5 shows our scaffolds that are between 25–168 $Å^2$, indicating their diverse shapes and electron densities, which allow our scaffolds to be potential biological modulators over a wide gamut of therapeutic targets.[16]

Another objective of this investigation was to develop strategies to synthesize compounds that have the potential to be biologically active. We understand that it is unrealistic to expect to generate bioactive molecules by using synthetic methods that are not directed towards any biological target. At the same time we hoped that our molecules may provide hits that are useful for further elaboration into drug leads. Pyrrolidinone, quinolizidinone and piperidinone frameworks randomly feature in natural products, which show antibacterial activity. Therefore, we decided to screen our compounds against five bacterial strains, *Pseudomonas aeruginosa*, *Klebsiella pneumonia*, *Staphylococcus aureus*, *Enterococcus faecalis* and *Escherichia coli*. Anti-microbial activity was determined by the well diffusion method as per the National Committee for Clinical Laboratory Standards [National Committee for Clinical Laboratory Standards (NCCLS), 1993, Performance Standards for effects Antimicrobial Disc Susceptibility Tests]. The pour plate method of microbial inoculation was conducted using 30 μl of microbial culture for 25–30 ml of Mueller–Hinton agar medium. Wells of 5 mm diameter were punched using a borer, and our molecules (0.2 mg dissolved in 20 μl of DMSO) were added to each well. The wells containing the solvent DMSO served as negative controls and Ciprofloxacin was used as a positive control. The plates were incubated at 37 °C for 24 h. The anti-microbial activity of the compounds was assessed by measuring the diameter (mm) of the zone of inhibition around the well and by calculating

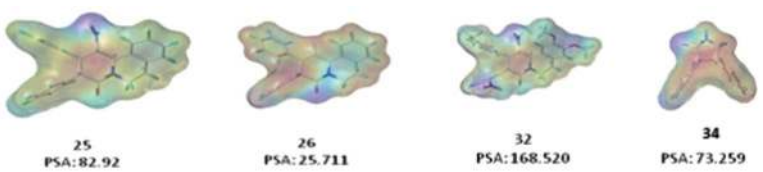

Fig. 5 Polar surface area (PSA) of our collection of molecules.

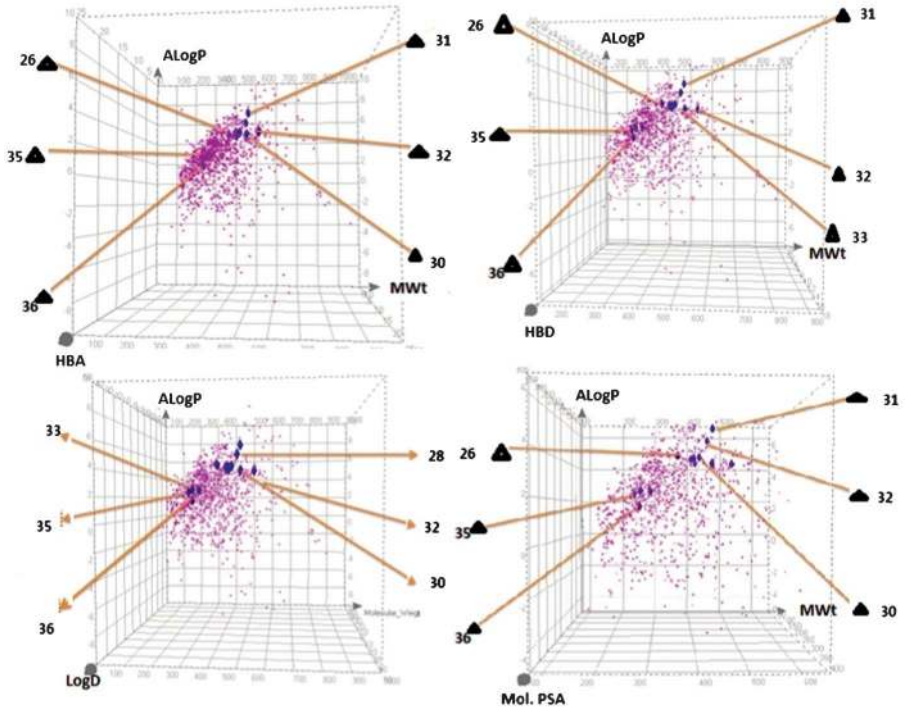

Fig. 6 Comparison of the *in silico* generated med-chem attributes between our compound selection and ~1000 FDA approved drugs.

the area of inhibition ($\pi R^2 - \pi r^2$, where R is the radius of the zone of inhibition and r is the radius of the well).

Results obtained in the present study revealed that our tested compound collection possess potential antibacterial activity against *P. Aeruginosa*, *K.Pneumonia*, *S. Aureus*, *E. Faecalis* and *E. Coli* (Table 4). In general, our compound collection *viz.* **24**, **27**, **30**, **31**, **32**, **33** and **35** showed significant activity against *P. Aeruginosa*. The highest activity of 20 mm was exhibited by **32** and the lowest of 10 mm by **31** and **27**. Compound **24**, **32** and **33** were active against *K. Pneumonia*, with the highest activity of 15 mm exhibited by **33**. Piperidinone **27** and the unsaturated quinolizidinone **32** along with pyrrolidinones **34** and **35** also exhibited activity against *E. Faecalis*. **32** showed a varied zone of inhibition from 7 mm to 20 mm against all the tested bacteria. The relative inactivity of our molecules against the pathogens *S. Aureus* and *E. Coli* indicates selective inhibition (**32**, which is the most active in our collection, shows an activity of 10 mm in both).

As indicated in the table above, among the molecules in our collection **24**, **32**, **33** and **35** showed significant activity against various bacterial species. This is further illustrated in Table 5 containing the MIC (minimum inhibitory concentration)/MBC (minimum bactericidal concentration) of our compounds, which were determined on the organisms that showed maximum susceptibility to our compounds. Even though this is not a medicinal chemistry study, these results do establish that this is a viable strategy for the rapid access of architecturally diverse scaffolds suitable for biological screen-

Table 4 Antibacterial activity of our compounds against bacterial species tested by a well diffusion assay

Diameter (mm)/zone (mm^2) of inhibition					
Microrganism Compounds	*P. Aeruginosa*	*K. Pneumoniae*	*S. Aureus*	*E. Faecalis*	*E. Coli*
24	12.1/93.3	10/58.9	8/18.8	9/43.9	8/30.6
27	10.1/58.9	—	—	7.1/18.9	—
28	9.4/43.8	—	8.5/37.1	8.1/30.6	7.1/18.8
29	9.5/51.2	—	7/18.8	8.4/31.2	—
30	—	—	—	6.1/8.6	9.1/58.9
31	10.2/58.9	—	7.3/18.9	7.1/18.8	7.4/19.2
32	20/294.4	12/93.4	7/18.8	13/113.1	10.1/58.9
33	14/134.2	15/157.0	8.1/30.6	12/93.4	9.1/43.9
35	11/75.4	—	6.9/18.6	14/134.2	—
37	9/43.9	—	—	10/58.9	—
Ciprofloxacin	14.02/134.2	15.03/157.1	14/134.2	13.4/113.0	19.2/283.4

Table 5 Determination of MIC and MBC by the tube dilution method

Compounds	Organism	MIC (mM)	MBC (mM)
24	*P. Aeruginosa*	1.58 ± 0.1	3.16 ± 0.15
27	"	1.62 ± 0.1	3.24 ± 0.16
28	"	0.63 ± 0.03	2.52 ± 0.12
29	"	0.76 ± 0.03	3.04 ± 0.15
31	"	0.61 ± 0.03	2.44 ± 0.12
32	"	0.83 ± 0.02	3.32 ± 0.16
33	"	1.56 ± 0.08	3.12 ± 0.15
30	*E. Coli*	1.40 ± 0.07	2.8 ± 0.14
35	*E. Faecalis*	1.45 ± 0.07	2.91 ± 0.14
37	"	0.62 ± 0.03	1.24 ± 0.06

ings, which can provide activities ideal for further investigation as potential lead compounds for med-chem programmes.

Conclusion

In summary, we have developed an efficient $TiCl_4$ catalyzed method for the Michael addition of Evans oxazolidinones with nitro olefins. We have also demonstrated a catalytic asymmetric version of this reaction with good yields and decent diastereoselectivity. To evaluate the potential of these nitro adducts as building blocks for diversity oriented synthesis (DOS) they were further converted to biologically relevant heterocycles *viz.* quinolizidinones, piperidinones and pyrrolidinones under facile reaction conditions. *In silico* analysis is utilized to evaluate the diversity of the set of compounds against shape space (PMI), polar surface area (PSA) calculations and relevant drug like properties (*viz.* HBA, HBD, PSA, mol. wt., log P and Log D). Finally, the molecules were screened against microorganisms to assess their biological activity.

Acknowledgements

The authors acknowledge GVK Bioscience for the funding.

References

1 (*a*) M. D. Burke and S. L. Schreiber, *Angew. Chem., Int. Ed.*, 2004, **43**, 46–58; (*b*) A. L. Hopkins and C. R. Groom, *Nat. Rev. Drug Discovery*, 2002, **1**, 727–730; (*c*) J. Drews and S. Ryser, *Nat. Biotechnol.*, 1996, **14**, 1516–1518; (*d*) H. An, S. -J. Eum, M. Koh, S. K. Lee and S. B. Park, *J. Org. Chem.*, 2008, **73**, 1752–1761; (*e*) D. B. Ramachary, C. Venkaiah, Y. V. Reddy and M. Kishore, *Org. Biomol. Chem.*, 2009, **7**, 2053–2062.

2 (*a*) W. R. J. D. Galloway, A. Bender, M. Welch and D. R. Spring, *Chem. Commun.*, 2009, 2446–2462; (*b*) W. R. J. D. Galloway and D. R. Spring, *Expert Opin. Drug Discovery*, 2009, **4**, 467–472; (*c*) W. R. J. D. Galloway, A. I. -Llobet and D. R. Spring, *Nat. Commun.*, 2010, 1–13.

3 (*a*) T. E. Nielsen and S. L. Schreiber, *Angew. Chem., Int. Ed.*, 2008, **47**, 48–56; (*b*) H. Oguri and S. L. Schreiber, *Org. Lett.*, 2005, **7**, 47–50.

4 (*a*) M. D. Burke, E. M. Berger and S. L. Schreiber, *Science*, 2003, **302**, 613–618; (*b*) R. J. Spandl, A. Bender and D. R. Spring, *Org. Biomol. Chem.*, 2008, **6**, 1149–1158.

5 (*a*) W. M. Golebiewski and I. D. Spenser, *Can. J. Chem.*, 1988, **66**, 1734–1748; (*b*) E. E. van Tamelen and R. L. Foltz, *J. Am. Chem. Soc.*, 1969, **91**, 7372–7377; (*c*) D. H. Hua, *Synthesis*, **191**, 970–974; (*d*) D. Lesma, *Eur. J. Org. Chem.*, 2001, 1377–1383; (*e*) T. Gallagher and D. Gray, *Angew. Chem., Int. Ed.*, 2006, **45**, 2419–2423; (*f*) L. Mandell, *J. Am. Chem. Soc.*, 1963, **85**, 2683–2684; (*g*) J. Chen, *J. Chem. Soc., Chem. Commun.*, 1986, 905–907; (*h*) S. Z. Zard, *Angew. Chem., Int. Ed.*, 1998, **37**, 1128–1131; (*i*) R. H. Robson and L. F. Prescott, *Br. J. Clin. Pharmacol.*, 1979, **7**, 81–87; (*j*) D. P. Rainey, E. B. Smalley, M. H. Crump and F. M. Strong, *Nature*, 1965, **205**, 203–204; (*k*) C. W. Robinson and K. A. Woerpel, *J. Org. Chem.*, 1999, **64**, 1434–1435; (*l*) H. Krawczyk, L. Albrecht, J. Wojciechowski, W. M. Wolf, U. Krajewska and M. Rozalski, *Tetrahedron*, 2008, **64**, 6307–6314; (*m*) R. K. Dieter and K. Lu, *Tetrahedron Lett.*, 1999, **40**, 4011–4014; (*n*) S. Berlin, C. Ericsson and L. Engman, *J. Org. Chem.*, 2003, **68**, 8386–8396; (*o*) C. Escolano, M. Amat and J. Bosch, *Chem.–Eur. J.*, 2006, **12**, 8198–8207; (*p*) O. Bassas, N. Lior, M. M. M. Santos, R. Griera, E. Molins, M. Amat and J. Bosch, *Org. Lett.*, 2005, **7**, 2817–2820.

6 (*a*) R. Smith, *Tetrahedron*, 1979, **35**, 437–489; (*b*) R. Smith, *Phytochemistry*, 1983, **22**, 1055–1056; (*c*) R. G. Arrayás, A. Alcudia and L. S. Liebeskind, *Org. Lett.*, 2001, **3**, 3381–3383.

7 (*a*) M. A. Katzman, *CNS Drugs*, 2009, **23**, 103–120; (*b*) I. M. Anderson, *J. Affective Disord.*, 2000, **58**, 19–36; (*c*) S. A. Montgomery, *Int. Clin. Psychopharmacol.*, 2001, **16**, 169–178; (*d*) D. E. Griswold, E. F. Webb, J. Breton, J. R. White, P. J. Marshall and T. J. Torphy, *Inflammation*, 1993, **17**(3), 333–344; (*e*) H. Wachtel, *Neuropharmacology*, 1983, **22**(3), 267–272; (*f*) C. R. Maxwell, S. J. Kanes, T. Abel and S. J. Siegel, *Neuroscience*, 2004, **129**(1), 101–107; (*g*) S. J. Kanes, J. Tokarczyk, S. J. Siegel, W. Bilker, T. Abel and M. P. Kelly, *Neuroscience*, 2006, **144**(1), 239–246.

8 (*a*) D. C. Rees, M. Congreve, C. W. Murray and R. Carr, *Nat. Rev. Drug Discovery*, 2004, **3**, 660–665; (*b*) M. Congreve, R. Carr, C. W. Murray and H. Jhoti, *Drug Discovery Today*, 2003, **8**, 876–879.

9 (*a*) S. Albrecht, J-M. Adam, U. Bromberger, R. Diodone, A. Fettes, R. Fischer, V. Goeckel, S. Hildbrand, G. Moine and M. Weber, *Org. Process Res. Dev.*, 2011, **15**, 503–514; (*b*) M. Böhringer, H. Fischer, M. Hennig, D. Hunziker, J. Huwyler, B. Kuhn, B. M. Loffler, T. Lubbers, P. Mattei, R. Narquizian, E. Sebokova, U. Sprecher and H. P. Wessel, *Bioorg. Med. Chem. Lett.*, 2010, **20**, 1106–1109; (*c*) M. Bohringer, B. Kuhn, T. Lubbers, P. Mattei, R. Narquizian, H. P. Wessel (F. Hoffmann-La Roche AG). *U.S. Pat. Appl. 2004/0259902*, 2004.

10 (*a*) C. E. Katz and J. Aube, *J. Am. Chem. Soc.*, 2003, **125**, 13948–13949; (*b*) M. Kenji, *Tetrahedron: Asymmetry*, 2005, **16**, 685–692; (*c*) M. -A. Kim, J. Y. Kim, K. -S. Song, J. Kim and J. Lee, *Tetrahedron*, 2007, **63**, 12845–12852; (*d*) Refer

the experimental; (*e*) D. A. Evans, T. C. Britton, R. L. Dorow and J. F. Dellaria, *Tetrahedron*, 1988, **44**, 5525–5540.
11 (*a*) P-Q. Huang, Z-Q. Guo and Y-P. Ruan, *Org. Lett.*, 2006, **8**(7), 1435–1438; (*b*) S. M.-C. Pelletier, P. C. Ray and D. J. Dixon, *Org. Lett.*, 2009, **11**(20), 4512–4515; (*c*) F. Xu, E. Corley, J. A. Murry and D. M. Tschaen, *Org. Lett.*, 2007, **9**(14), 2669–2672; (*d*) P. S. Hynes, P. A. Stupple and D. J. Dixon, *Org. Lett.*, 2008, **10**(7), 1389–1391.
12 Please refer to the NOE in the experimental section.
13 (*a*) GVK Bioscience proprietary database; (*b*) Stable 3D structures of all compounds were used to calculate their physicochemical properties, such as molecular weight, number of hydrogen-bond donors (HBD), number of hydrogen bond acceptors (HBA), ALogP, LogD and polar surface area (PSA), these values were calculated by using Discovery Studio 3.1 (Accelrys Inc.).
14 W. H. B. Sauer and M. K. Schwartz, *J. Chem. Inf. Model.*, 2003, **43**, 987–1003.
15 GVKBio proprietary software.
16 H. Pajouhesh and G. R. Lenz, *NeuroRx*, 2005, **2**, 541–553.